



Inter Satellite Omnidirectional Optical Communication for Cube-Satellite Crosslink

Ozdal Boyraz, Ph.D.

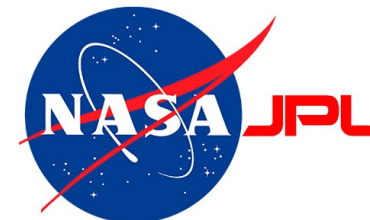
University of California, Irvine

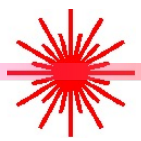
Jose E. Velazco, Ph.D.

JPL



This presentation has been approved for public release





Omnidirectional Inter-satellite Optical Communicator

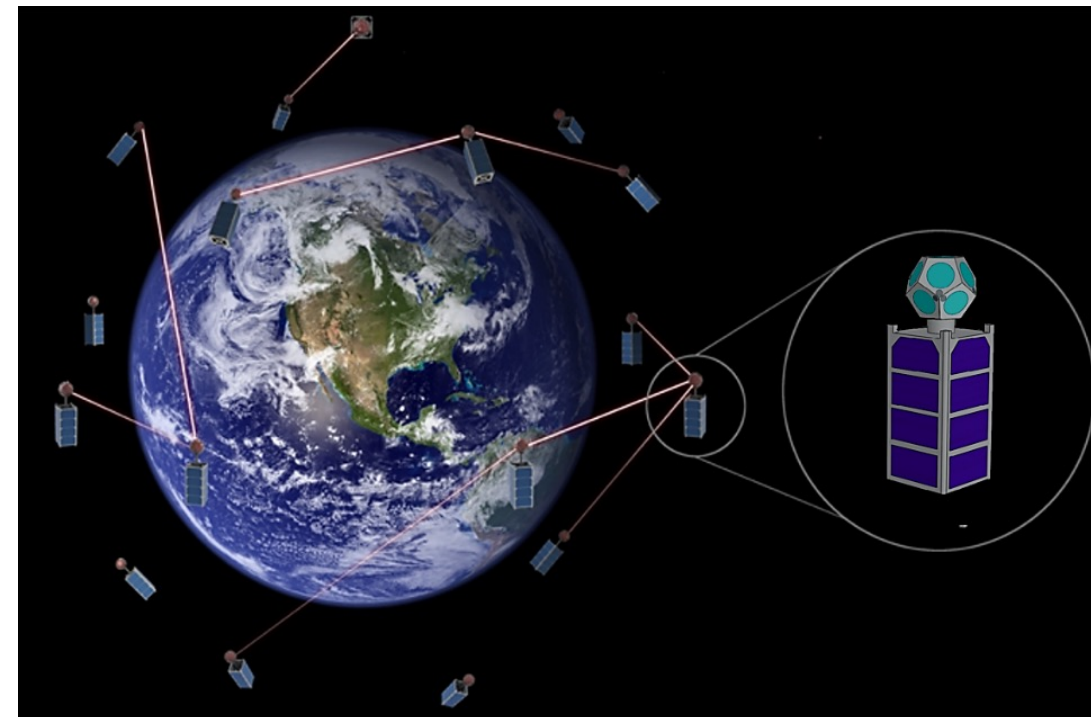
Univ. PI: Ozdal Boyraz, University of California, Irvine

NASA POC: Dr. Jose Velazco, JPL

Project Summary

- **HQ Directorate:** STMD
- **PI:** Ozdal Boyraz, University of California Irvine
- **Co-Is:** Dr. Jose Velazco, JPL

Description: : Advanced omnidirectional inter-satellite optical communicator is being proposed to enable high bandwidth, full duplex optical communication between small spacecraft. In particular, the proposal aims at space, power and performance challenges pertinent to CubeSat mission. The Omnidirectional Inter-Satellite Optical Communicator (ISOC) project is managed by the Small Spacecraft Technology Program (SSTP), which is chartered to develop and mature technologies to enhance and ^[1]expand the capabilities of small spacecraft with a particular focus on communications, propulsion, pointing, power, and autonomous operations.



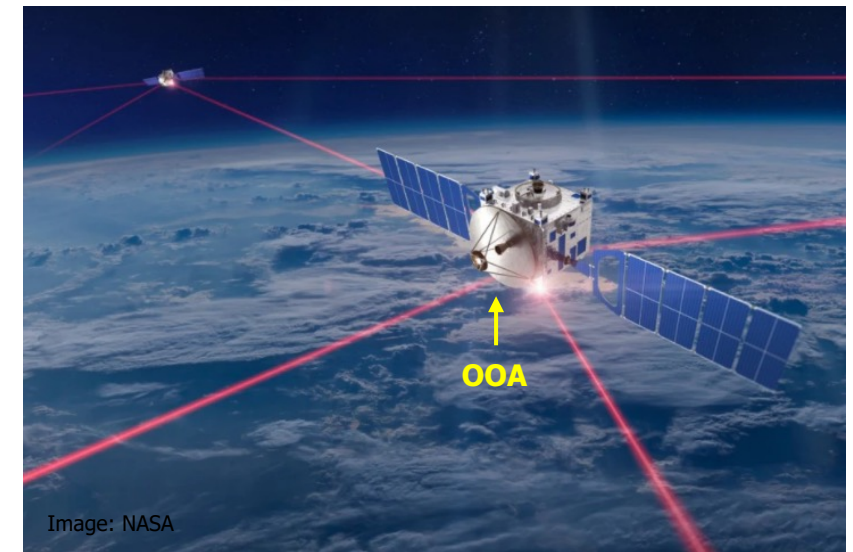
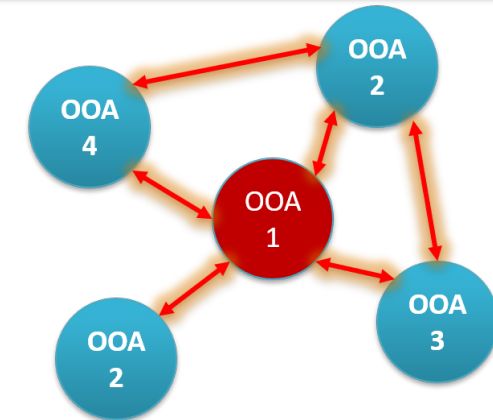


Outline

- ❑ Inter Satellite Omnidirectional Optical Communication
 - Sph
 - Wavelength Selective Optical Transceiver
 - Jitter and Receiver
 - Transmitter
 - Lab Work
- ❑ Multi-Tone Continuous Wave Lidar
 - Motivation
 - Target Applications
 - Concept
 - Experimental results

Omnidirectional Optical Communication

- ❑ CubeSat constellation demand for high-speed crosslink.
- ❑ Up to date, microwave crosslink data rate is limited to less than 80 Mb/s. (in 180 kg satellite platform)
- ❑ Optical communication can provide multi-Gigabits/s crosslink.
- ❑ To the best of our knowledge, all the research work on the satellite optical link have been done either for satellites with significantly less SWaP-C constraints or for a single point-to-point data communication.
- ❑ The optical communication between CubeSats with more stringent SWaP-C limits is a relatively new area of research.

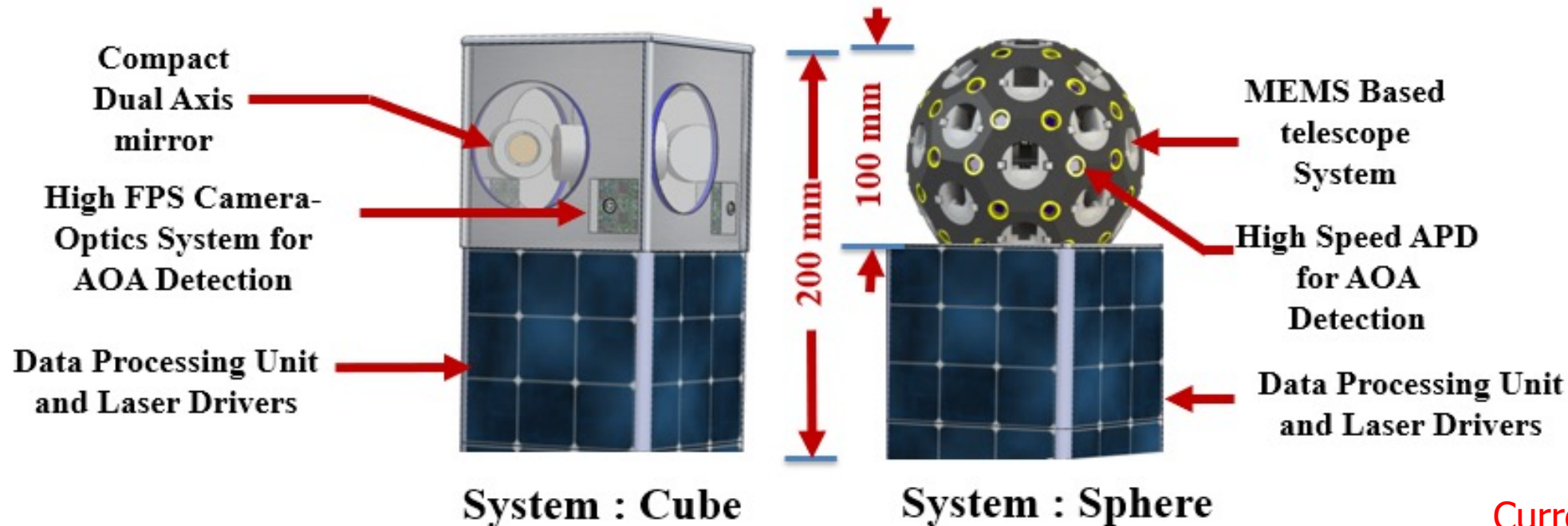


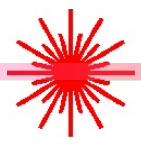
Feasibility of **omnidirectional optical communication** in a CubeSat platform is a new concept that needs to be investigated.

Omnidirectional optical crosslink in a CubeSat platform is still an open area of research.

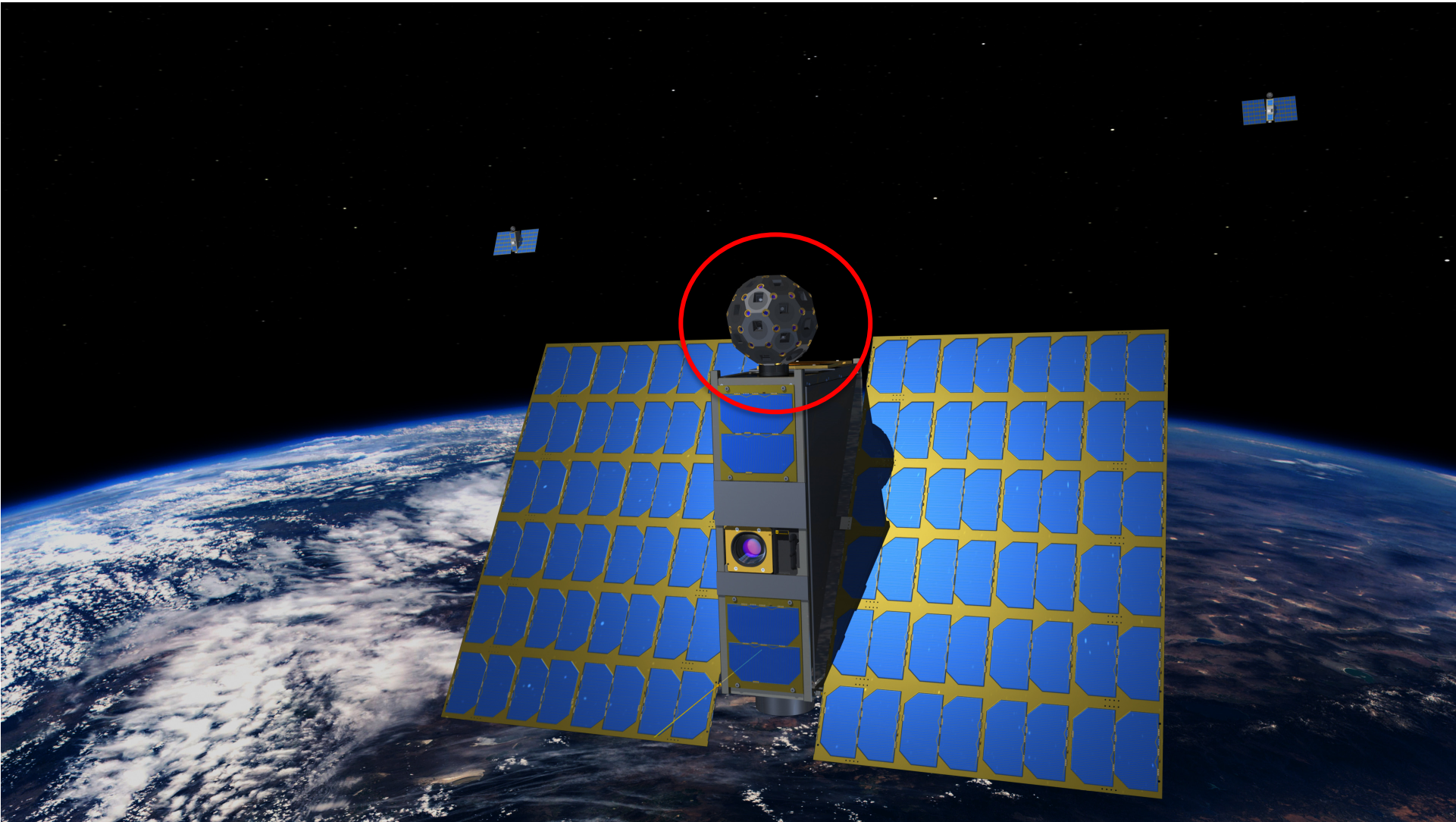
Developed Technologies

- ❑ Two separate configurations has been studied
- ❑ All components are commercially available off the shelf components or based on commercially available components
- ❑ JPL leads the first effort, and it is in implementation phase
- ❑ UCI leads the wavelength selective optical system with dual axis mirrors

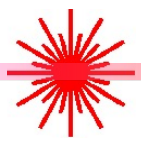




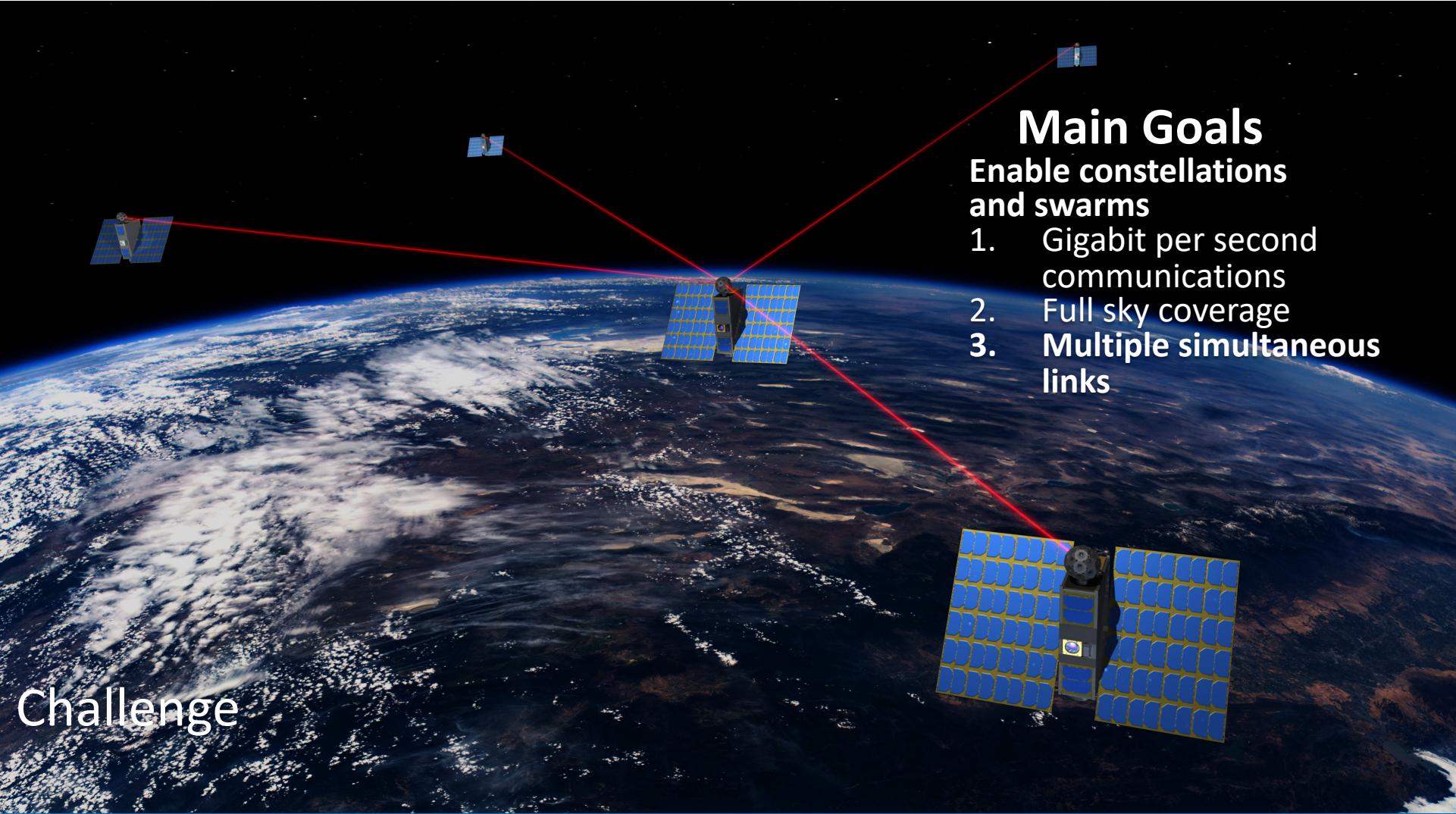
1. Introduction



Description of ISOC: **Inspiration**



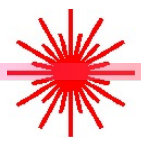
1. Introduction



Main Goals

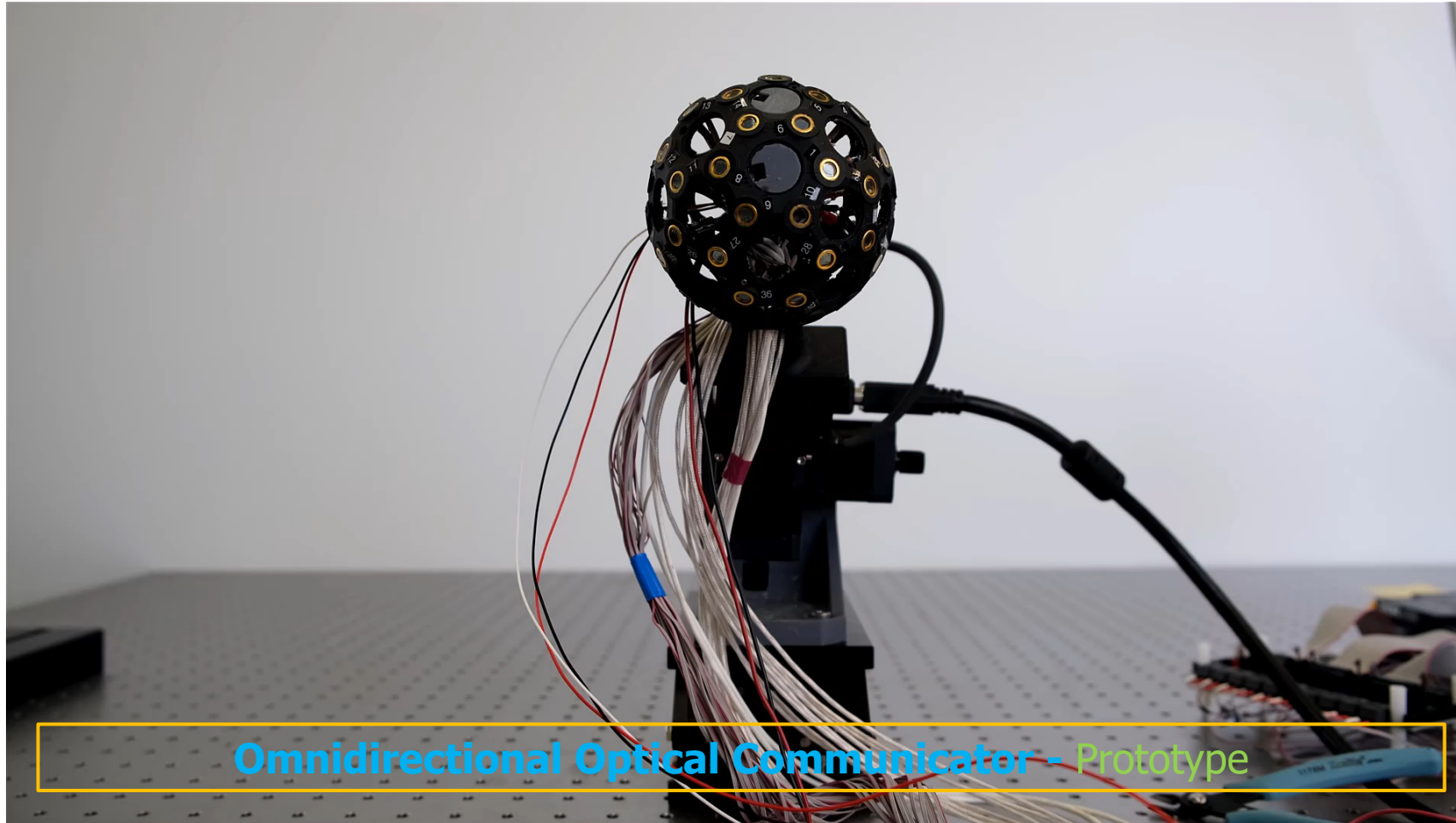
- Enable constellations and swarms
1. Gigabit per second communications
 2. Full sky coverage
 3. **Multiple simultaneous links**

Description of ISOC: Challenge



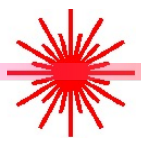
1. Introduction

Let me introduce to you the ISOC:



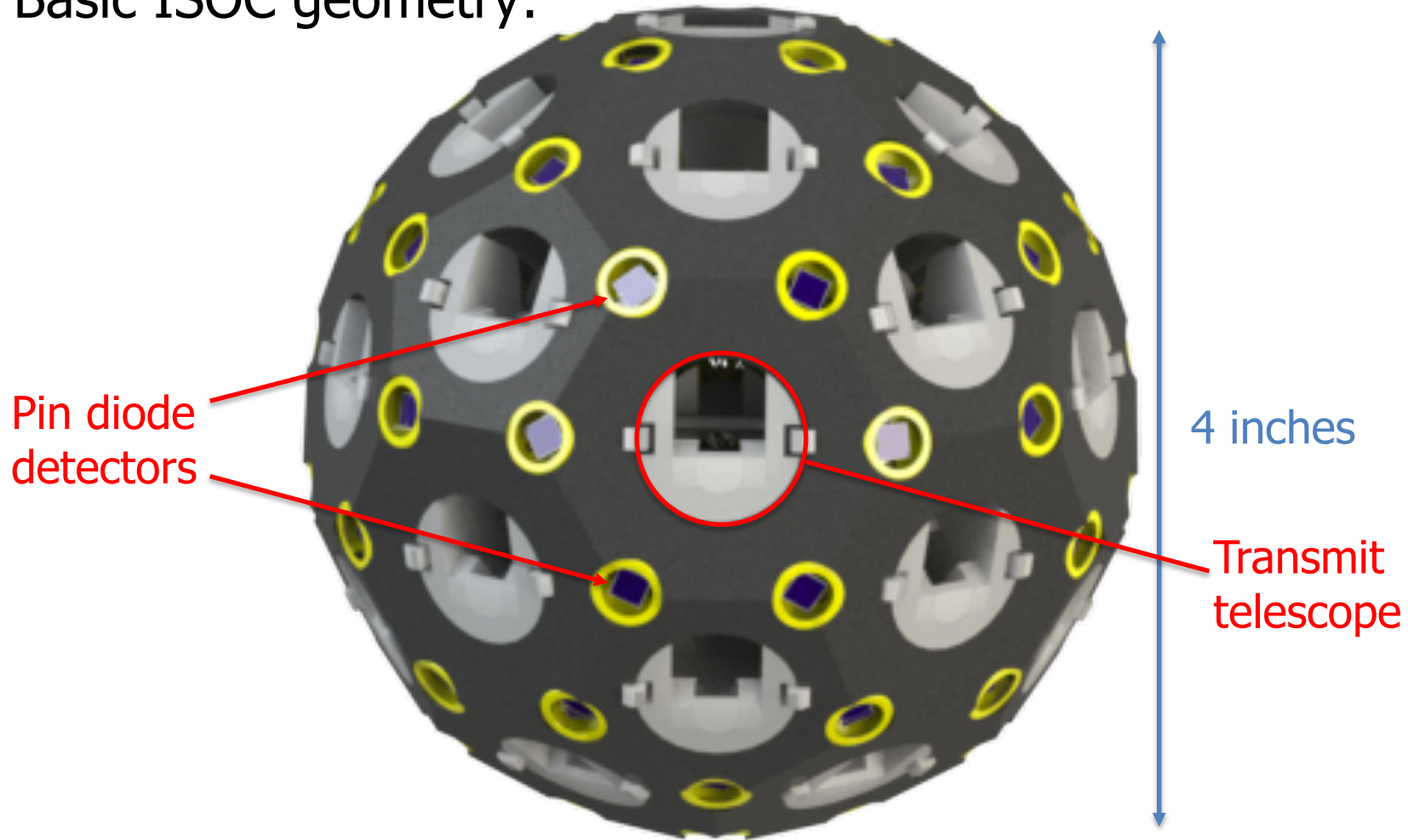
Omnidirectional Optical Communicator - Prototype

Description of ISOC: [ISOC Introduction](#)

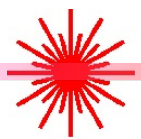


1. Introduction

Basic ISOC geometry:



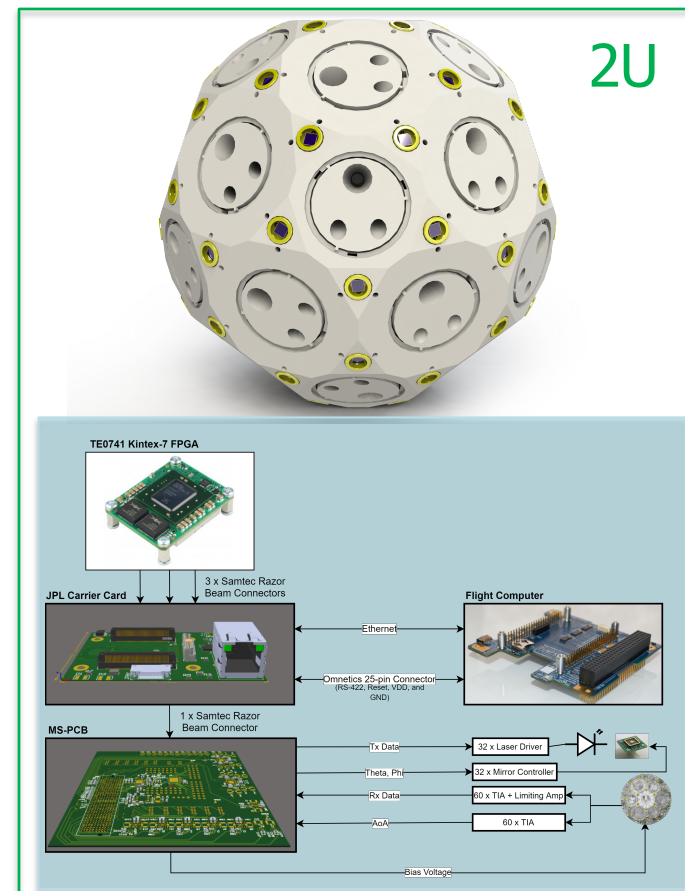
Description of ISOC: **Basic ISOC geometry**

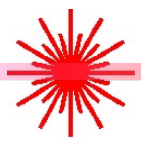


2. ISOC Testing

ISOC Flight Model

| ISOC Parameters | |
|------------------------------|---------|
| Parameter | Value |
| Wavelength | 850 nm |
| Optical Tx Power (per laser) | 1 W |
| Transmit diameter | 0.5 cm |
| Receive diameter | 1 cm |
| Data rate (≤ 200 km) | 1 Gbps |
| Power Usage | 15 W |
| Volume | 1.5U |
| Mass | 0.75 kg |

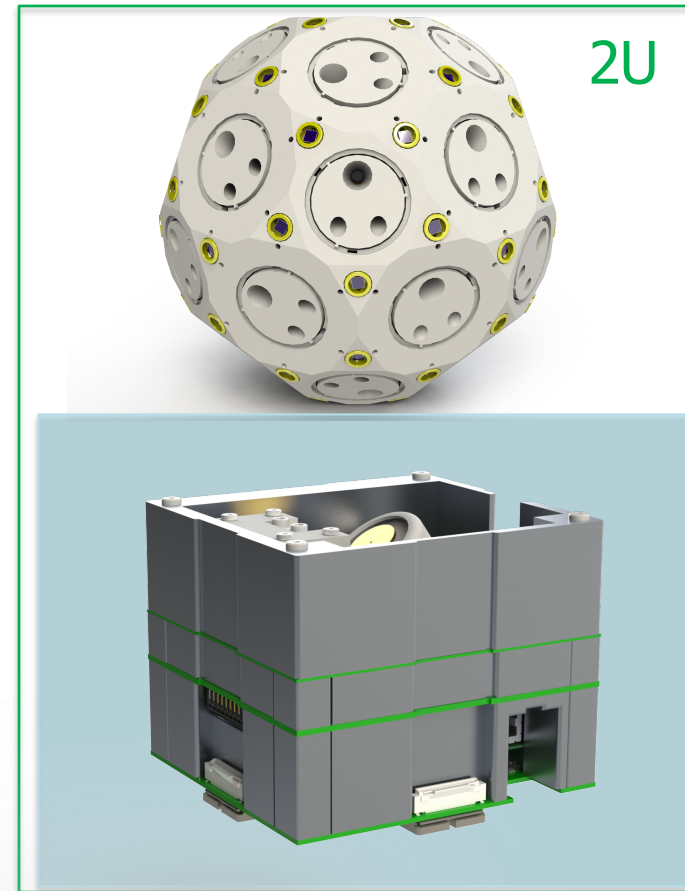


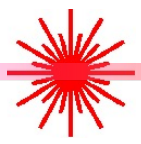


3. Technologies for INSPIRE

ISOC Flight Model

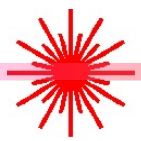
| ISOC Parameters | |
|------------------------------|---------|
| Parameter | Value |
| Wavelength | 850 nm |
| Optical Tx Power (per laser) | 1 W |
| Transmit diameter | 0.5 cm |
| Receive diameter | 1 cm |
| Data rate (≤ 200 km) | 1 Gbps |
| Power Usage | 15 W |
| Volume | 1.5U |
| Mass | 0.75 kg |



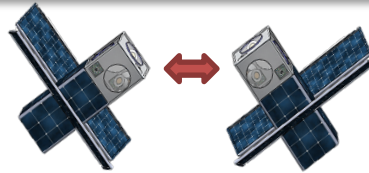


4. Conclusions

- A novel Omnidirectional Optical Communicator has been presented
- We presented design considerations and test results of the ISOC prototype developed under this SSTP project
- The ISOC is a potential enabler for future swarm and constellation missions



Wavelength Selective Optical Transceiver



Omnidirectional optical communicator design based on a CubeSat scale **Wavelength Selective Optical Transceiver (WSOT)** system architecture that can achieve 360° Field of Regard (FOR), more than 100 km communication distance, and higher than 400 Mb/s data rates.



The design and optimization rule for transmitter and receiver to achieve omnidirectionality.

A statistical pointing error model is derived that relates key receiver design parameters to the link performance.

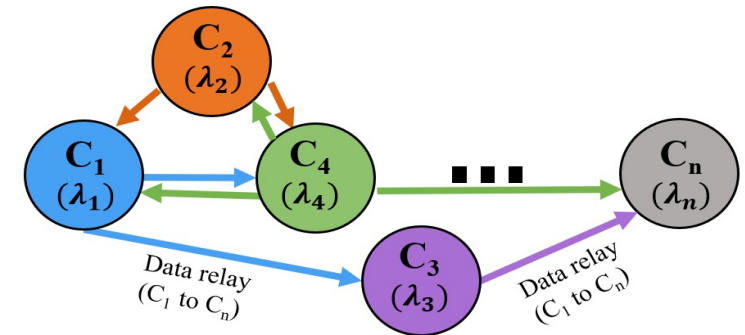
Practical Challenges

- ❑ The first practical challenges is the wavelength allocation, and eliminating cross talk due to back reflections
 - Wavelength selective approach has been investigated
- ❑ Power management
 - CW vs pulsed communication has been investigated
 - Impact of extinction ratio in pulsed modulation has been studied
 - Mode locked vs pulsed modulation has been compared
- ❑ Impact of pointing jitters has been studied for given receiver architectures
 - Metalens design has been proposed to mitigate the pointing jitter
- ❑ Finally, impact of aperture sizes for commercially available scanning mirrors has been evaluated

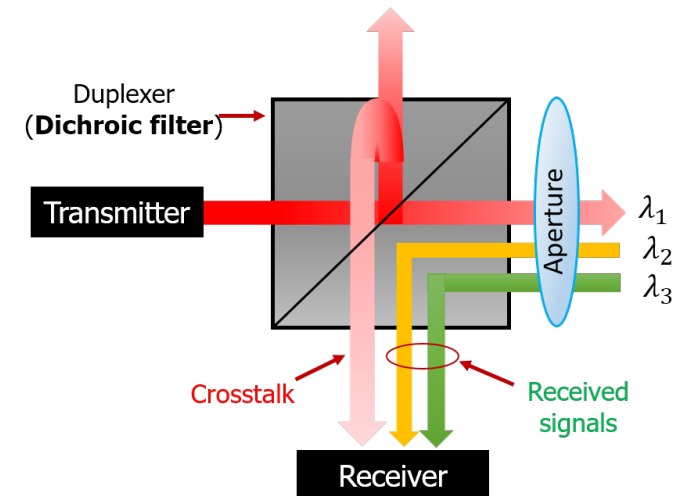
Advantage of WSOT

- ❑ Each WSOT transceiver of the CubeSat C_i incorporates an unique dichroic filter with center wavelength λ_i .
- ❑ By design, Dichroic filters **pass only one wavelength** and **-> reflects other wavelengths**.
- ❑ As a result, the C_i transmits signals with λ_i to other CubeSats $C_{j \neq i}$ but it can detect all other wavelengths, $\lambda \neq \lambda_i$.
- ❑ Experimentally, only **4 nW** crosstalk power is measured for a transmit power of **10.4 mW**. That is less than **0.0001%**.
- ❑ Hence WSOT system can increase the receiver sensitivity by suppressing the crosstalk component.
- ❑ Let's define crosstalk ratio , $C_T = \frac{\text{Crosstalk power}}{\text{Transmit power}}$.

- C_T is about **-65 dB** for a WSOT system whereas
- C_T is around **-30 dB** for a single wavelength-based system.
- Additionally, almost **zero received power loss** is measured.



WSOT based CubeSat constellation concept [1].

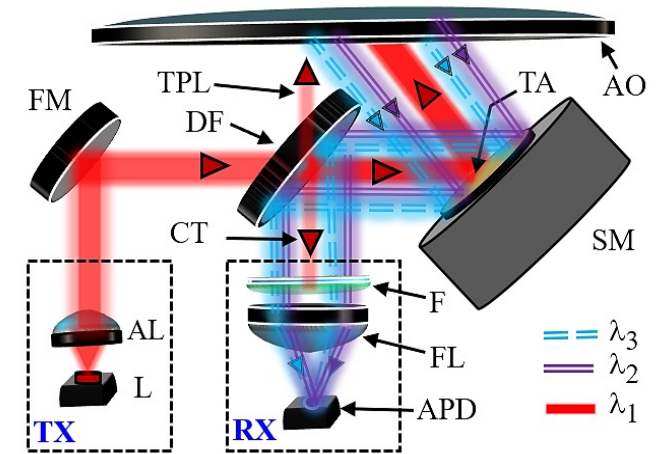


Dichroic filter as a duplexer.

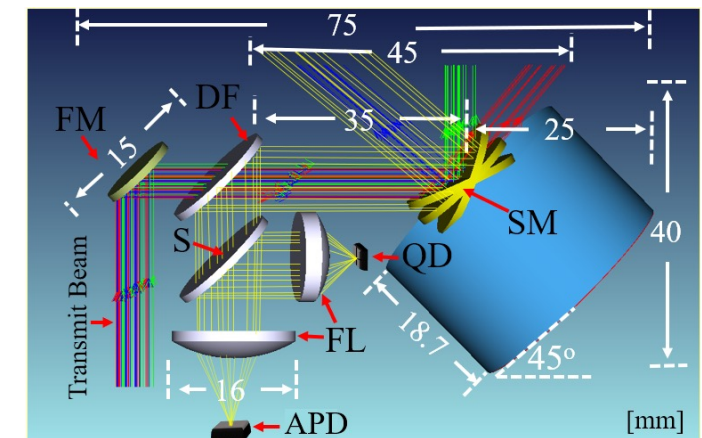
WSOT Architecture

- ❑ The transmitter (TX) chain incorporates,
 - A laser diode (L) -Aspheric lens (AL) -A fixed mirror (FM)
- ❑ WSOT receiver chain incorporates,
 - A wideband filter (F) -Focusing lens (FL) - photodetector (APD)
- ❑ A dichroic filter (DF) is incorporated that enables full-duplex communication and minimizes the crosstalk.
- ❑ A high-speed scanning mirror of 15 mm diameter is used as transceiver aperture (TA). Scanning mirror facilitates,
 - High FOR transmission -Direct line of sight communication
- ❑ Additionally, a beam sampler (S), a quad-detector (QD) is also required to facilitate the pointing and tracking.
- ❑ It is ensured that the entire transceiver can fit within 75 mm x 40 mm dimension to satisfy CubeSat SWaP constraints.

Up to six WSOT transceivers can fit inside less than 3U CubeSat i.e. 300 mm x 100 mm x 100 mm to establish omnidirectional communication.



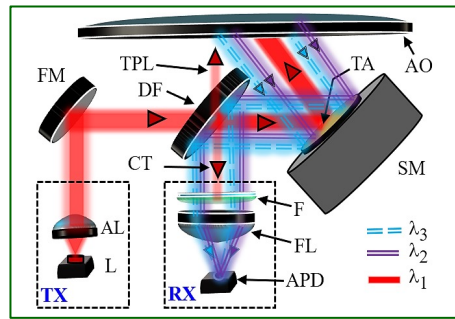
WSOT system [1]



WSOT dimension in millimeters [1]

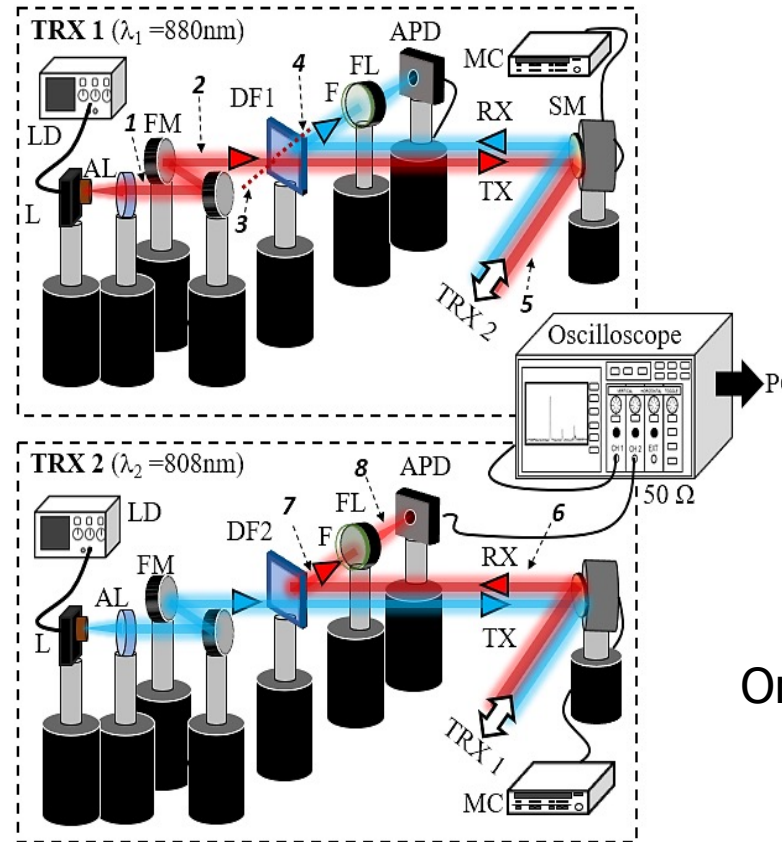
WSOT transceiver optical loss measurement

Two Flatsat models of WSOT is assembled to test the performance of the system.



WSOT system unit

DF: Dichroic Filter L: Laser
 FM: Fixed Mirror SM: Scanning Mirror
 AL: Aspheric Lens
 APD: Avalanche Photo Detector



WSOT system experimental setup [1].

TABLE I
 OPTICAL POWER LOSS OF THE WSOT TRANSCEIVER

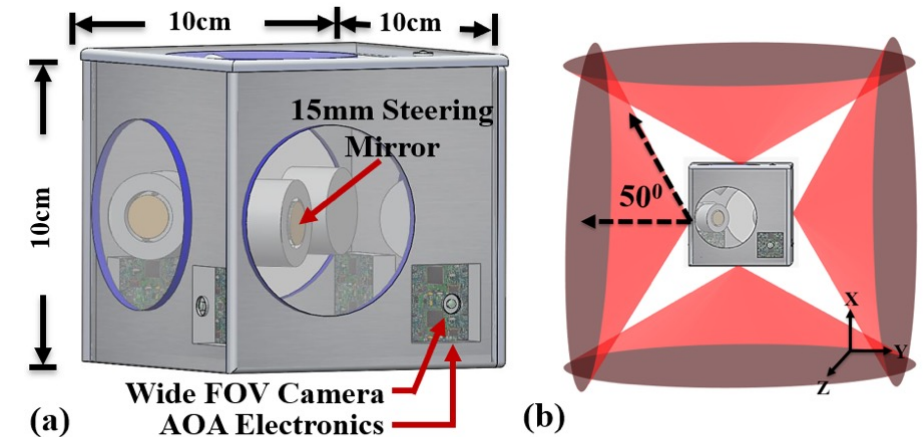
| Test points | Symbol | Description | Power Loss (dB) |
|-------------|----------------|------------------------------|-----------------|
| 1 | L_{AL} | Collimation loss | -0.2 |
| 2 | L_M | Mirror loss | -0.15 |
| 3 | L_{DF} | Dichroic filter loss | -0.12 |
| 4 | C_T | Crosstalk factor of DF | ≈ -65 |
| 5 | L_{TA1} | Scanning mirror loss (TRX1) | -0.18 |
| 6 | L_{TA2} | Scanning mirror loss (TRX2) | -0.18 |
| 7 | L_{DF} | Dichroic filter loss | -0.07 |
| 8 | $L_F + L_{FL}$ | Filter and lens loss | -0.7 |
| | L_{OCL} | Total optical component loss | -1.6 |

Only **1.6 dB** optical loss is measured in the WSOT system.

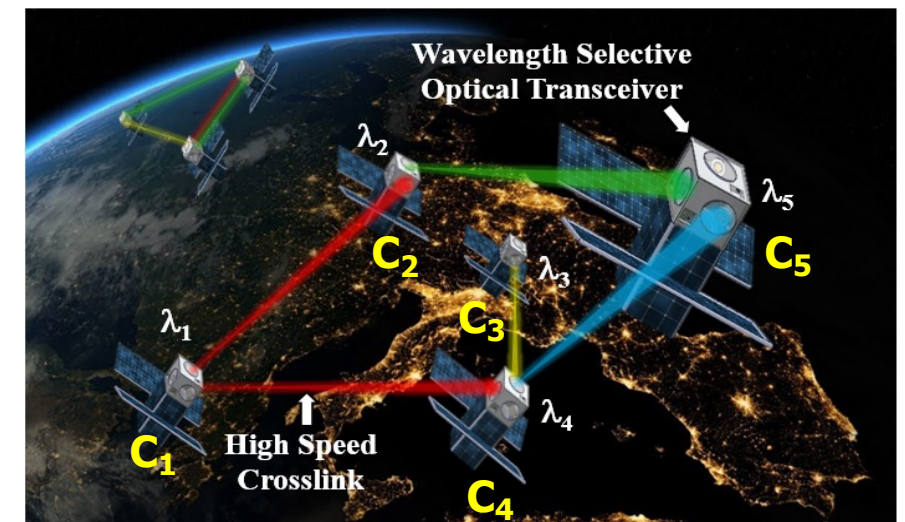
[1] I. U. Zaman, J. E. Velazco and O. Boyraz, "Realization of Omnidirectional CubeSat Crosslink by Wavelength-Selective Optical Transceiver," in *IEEE Journal on Miniaturization for Air and Space Systems*, vol. 1, no. 1, pp. 47-55, June 2020, doi: 10.1109/JMASS.2020.2995316.

WSOT Summary

- ❑ Omnidirectional CubeSat optical crosslink concept based on Wavelength Selective Optical Transceiver (WSOT).
- ❑ The mentioned proof-of-concept transceiver shows better than -28 dBm sensitivity for a bandwidth greater than 400 MHz.
- ❑ It is estimated that with only 15 mm transceiver aperture size and 1 W peak bit power, the system attains communication distance more than 125 km with a data rate of 400 Mb/s.
- ❑ A conservative Gaussian statistical computation of the BER is used. The actual communication BER is expected to be better than the estimated one.
- ❑ The performance of the system can be improved further by advanced receiver circuit design, error correction coding and optics optimization.



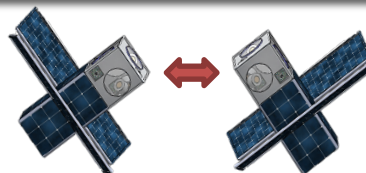
Omnidirectional Optical Communicator based on WSOT.



WSOT based CubeSat constellation concept.



Jitter Rejection Receiver Analytical Model



Omnidirectional optical communicator design based on a CubeSat scale **Wavelength Selective Optical Transceiver (WSOT)** system architecture that can achieve 360° Field of Regard (FOR), more than 100 km communication distance, and higher than 400 Mb/s data rates.

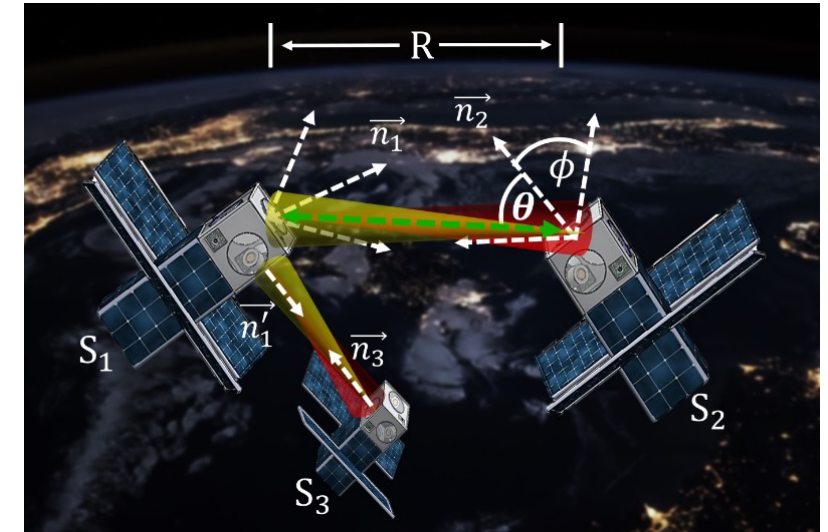
A statistical pointing error model is derived that relates key receiver design parameters to the link performance[1].

The design and optimization rule for transmitter and receiver to achieve omnidirectionality.

[1] I. U. Zaman and O. Boyraz, "Impact of receiver architecture on small satellite optical link in the presence of pointing jitter," *Appl. Opt., AO*, vol. 59, no. 32, pp. 10177–10184, Nov. 2020 (**OSA Spotlight, December 2020**)

Receiver architecture model

- ❑ The initial link is usually established with the help of Ephemerides data and the advanced PAT system [1,2]. ->
- ❑ The AOI θ varies based on the satellite orientation. However, data communication requires, $\theta < \phi$.
- ❑ The pointing jitter is always present.
- ❑ The instantaneous AOI at the receiver optical aperture,



Satellite constellation operates with pointing jitters [1].

$$\theta_i = \theta + \theta_T$$

Instantaneous AOI θ_i is the sum of the slowly varying AOI θ and the pointing jitter θ_T .

- ❑ For a given θ , The instantaneous received optical power by the receiver can be written as,

$$P_{rcv}(\theta_T) = P_T G_A \alpha L_p \left(\frac{\lambda}{4\pi R} \right)^2 L_{PJ}(\theta_T)$$

Instantaneous received power by the aperture

Transmit power P_T

Antenna Gain G_A

Transceiver loss α

Pointing Loss L_p

Distance R

Power loss at the aperture due to pointing jitter $L_{PJ}(\theta_T)$

AOI: Angle of Incidence

[1] Chang et. al., "Body pointing, acquisition and tracking for small satellite laser communication," in Free-Space Laser Communications XXXI, Mar. 2019, vol. 10910.

[2] Scheinfeld et. al, "Acquisition system for microsatellites laser communication in space," in Free-Space Laser Communication Technologies XII, May 2000, vol. 3932, pp. 166–175.

Receiver architecture model

- The instantaneous signal photocurrent,

$$i_{PD}(\theta, \theta_T, S) = R_\lambda G P_{rcv}(\theta_T) \cdot K(\theta, \theta_T, S)$$

Performance degradation factor depends on **receiver architecture**

Responsivity $\rightarrow R_\lambda$
 Detector gain $\rightarrow G$
 Instantaneous received power by the aperture $\rightarrow P_{rcv}(\theta_T)$
 Performance degradation factor depends on **receiver architecture** $\rightarrow K(\theta, \theta_T, S)$

- The performance degradation parameter can be expressed as [1]

$$K(\theta, \theta_T, S) = \eta_{BO}(\theta, \theta_T, S) \eta_{AR}(\theta, \theta_T) \eta_\lambda(\theta, \theta_T) \eta_C(A)$$

Beam walk-off at the detector plane $\rightarrow \eta_{BO}(\theta, \theta_T, S)$
 Reflection due to AR coating $\rightarrow \eta_{AR}(\theta, \theta_T)$
 Angle dependent responsivity $\rightarrow \eta_\lambda(\theta, \theta_T)$
 Detector coupling efficiency $\rightarrow \eta_C(A)$

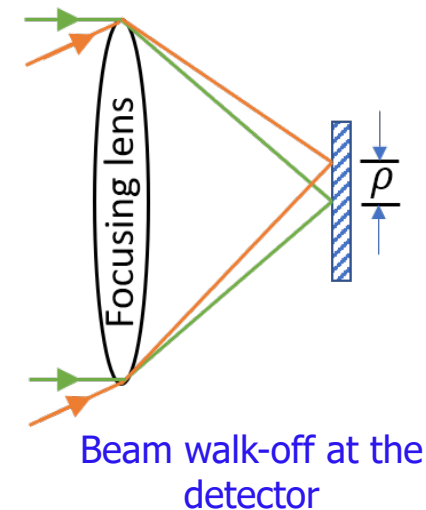
- All the terms depend on the instantaneous pointing jitters.
- In FSO communication, the focal spot size is comparable to the detector size.
- The **beam walk off** is the dominant factor.
- Considering only the dominant terms, the performance factor is given by

$$K(\theta, \theta_T, S) \approx \eta_{BO}(\theta, \theta_T, S) \eta_C(A).$$

FSO: Free Space Optical

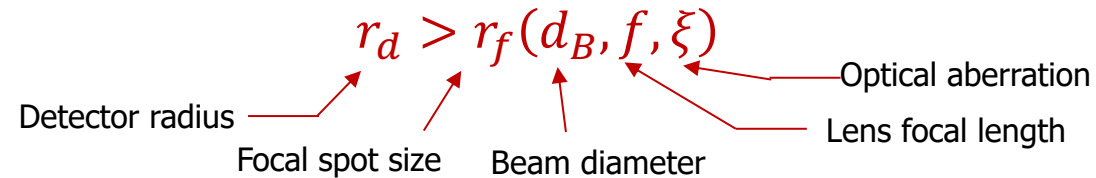
A, S : Set of receiver design parameters.

- Aperture size
- Detector size
- Lens focal length, etc.



Receiver architecture model

- Assume the photodetector's radius r_d is close to but larger than the focal spot radius r_f



- The performance degradation factor can be expressed as [1]

$$K(\theta, \theta_T, S) \approx \frac{0.318\eta_c(A)}{r_f(d_B, f, \xi)^2} \left(r_f(d_B, f, \xi)^2 \cos^{-1} \frac{\gamma_2}{r_f} + r_d^2 \cos^{-1} \frac{\gamma_1}{r_d} - \gamma_1 \sqrt{r_d^2 - \gamma_1^2} - \gamma_2 \sqrt{r_f(d_B, f, \xi)^2 - \gamma_2^2} \right)$$

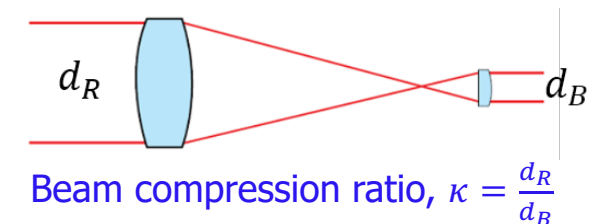
Detector coupling efficiency $\approx \eta_c(A)$ if $\rho(\kappa\theta, \kappa\theta_T) < r_d - r_f$
 ≈ 0 if $\rho(\kappa\theta, \kappa\theta_T) > r_d + r_f$

$$\gamma_1 = \frac{r_d^2 - r_f(d_B, f, \xi)^2 + \rho(\kappa\theta, \kappa\theta_T)^2}{2\rho(\kappa\theta, \kappa\theta_T)}$$

$$\gamma_2 = \frac{r_f(d_B, f, \xi)^2 - r_d^2 + \rho(\kappa\theta, \kappa\theta_T)^2}{2\rho(\kappa\theta, \kappa\theta_T)}$$

Radial displacement of the focal spot

Beam compression ratio



The degradation factor K largely depends on the receiver architecture

Sample architecture model

- ❑ The general formulation can be modified according to a specific receiver architecture.
- ❑ Let's consider a sample direct detection receiver. ->
- ❑ The performance degradation factor is reduced to [1]

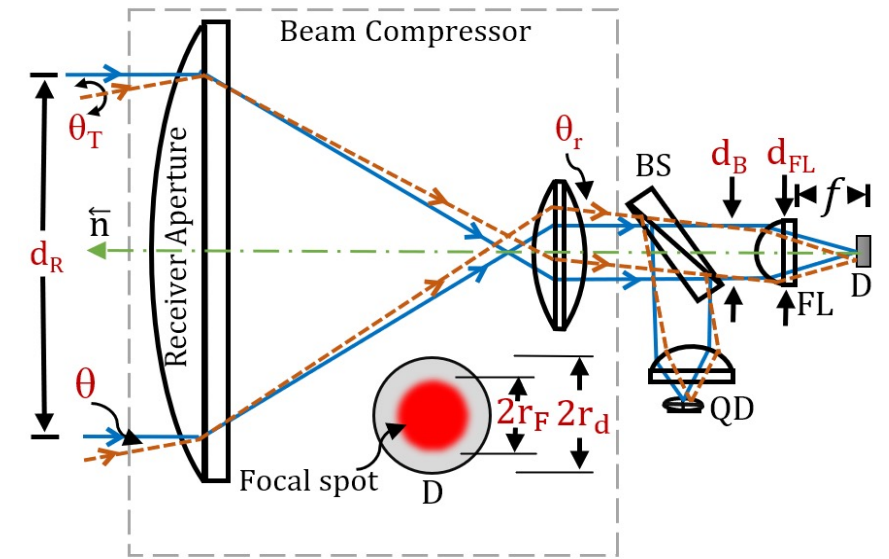
$$K_s(\theta_T, r_d, d_R, N, m_T, \xi, \tau) \approx \frac{1}{\pi} \sec^{-1} \left(\frac{2ABNd_R}{B^2 + A^2N^2d_R^2 - r_d^2} \right) + \frac{r_d^2}{B^2\pi} \sec^{-1} \left(\frac{2ANd_Rr_d}{-B^2 + A^2N^2d_R^2 + r_d^2} \right) - \frac{1}{B^2\pi} ANd_R \left[r_d^2 - \frac{(-B^2 + A^2N^2d_R^2 + r_d^2)^2}{4A^2N^2d_R^2} \right]^{0.5}$$

Pointing jitter $\rightarrow \theta_T$
 Detector radius $\rightarrow r_d$
 Aperture diameter $\rightarrow d_R$
 F-number of the FL $\rightarrow N$
 Beam compression ratio $\rightarrow m_T$
 Aberration factor $\rightarrow \xi$
 AOI to FOV ratio $\rightarrow \tau$

$$\approx 1 \text{ if } N \left(\frac{\tau r_d}{N} + d_R \theta_T \right) < r_d - B$$

$$\approx 0 \text{ if } N \left(\frac{\tau r_d}{N} + d_R \theta_T \right) > r_d + B$$

$$A = \theta_T + \frac{\tau r_d}{d_R N} \text{ and } B = 0.64N\lambda + \frac{d_R \xi}{2m_T N^2}$$



Sample direct detection optical receiver

d_R : aperture diameter
 d_B : beam diameter after the compressor
 r_f : focal spot radius
 θ_r : angular variation after the compressor
 BS: beam splitter
 QD: quad detector
 FL: focusing lens
 D: detector

$$N = \frac{\text{Focal length}}{\text{Diameter}}$$

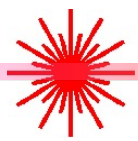
$$\tau = \frac{\text{Angle of incidence}}{\text{Receiver's FOV}} = \frac{\theta}{\phi}$$

$$m_T = \frac{d_R}{d_B}$$

[1] I. U. Zaman and O. Boyraz, "Impact of receiver architecture on small satellite optical link in the presence of pointing jitter," *Appl. Opt., AO*, vol. 59, no. 32, pp. 10177–10184, Nov. 2020



Proposal on Metalens Wide Angle Receiver Design

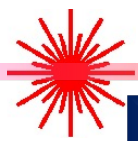


Motivation

- ❑ Field of view is a limiting factor for free space optical communication systems
- ❑ Optical telescopes and focusing optics concentrates light to detector for high efficiency detection within small field of view
- ❑ Beam walk off or pointing jitter often causes interruptions in communication systems or reduces the SNR
- ❑ Large area detector can ensure broader field of view, but it suffers from slow bandwidth

Objective

- ❑ To design a receiver such that broad field of view is achievable with reduced size of detector and without sacrificing beam compression ability
- ❑ Such system would reduce error from receiver misalignment with the transmitter in Free Space Optical Communication (FSOC)



Proposed System

- The proposed system consists of 2 axially symmetric metalenses (ML_1 , ML_2) with quadratic phase profile ($\exp(\frac{ik(x^2+y^2)}{2f})$) and 1 off-the-shelf aspheric lens
- Metalens 1 focuses incident optical beam on its focal plane. Different incident angle will be focused on different location in the focal plane
- Metalens 2 is on the focal plane of metalens 1. It makes the beam parallel to optical axis
- The aspheric lens focuses the parallel beams to the detector sitting on the optical axis

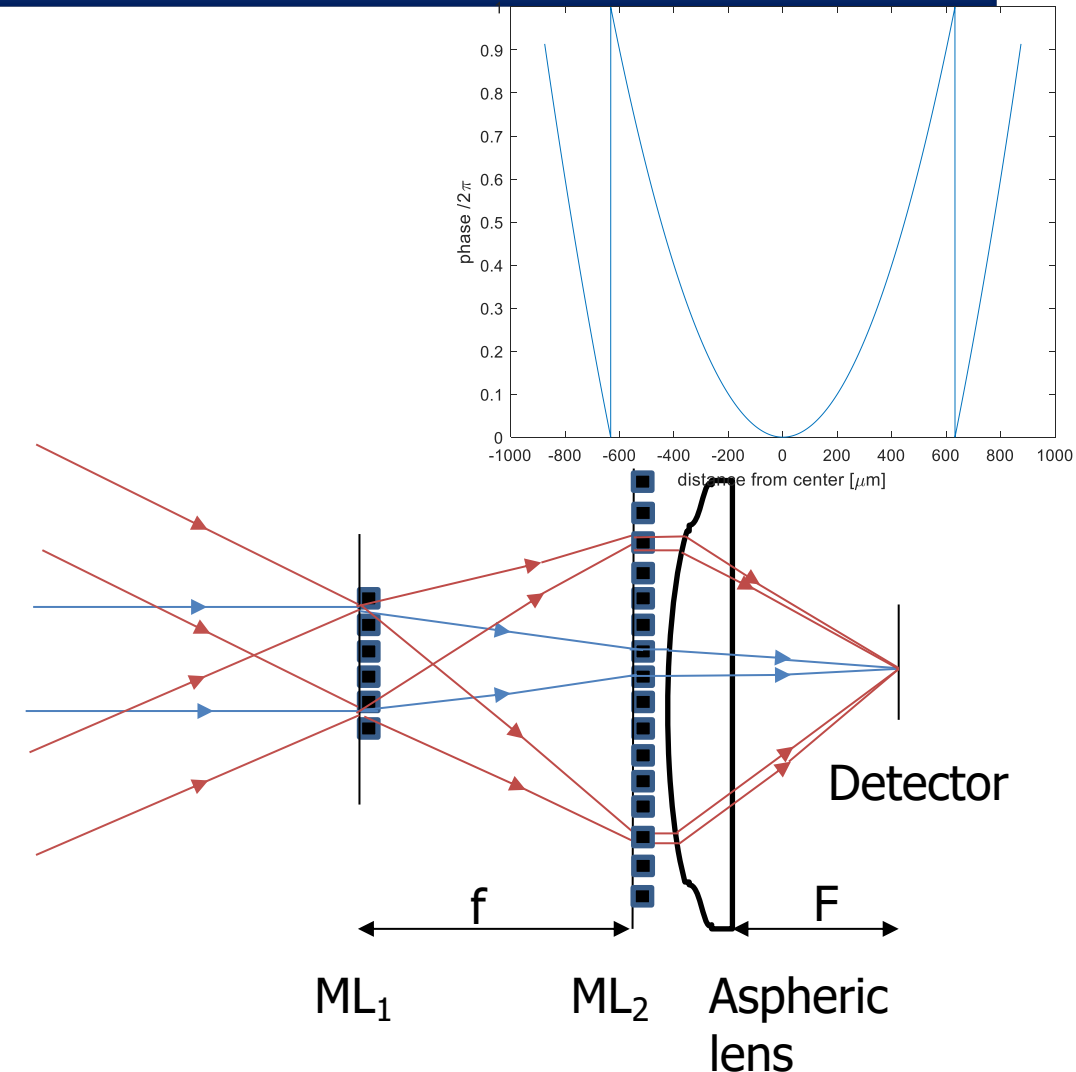
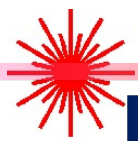
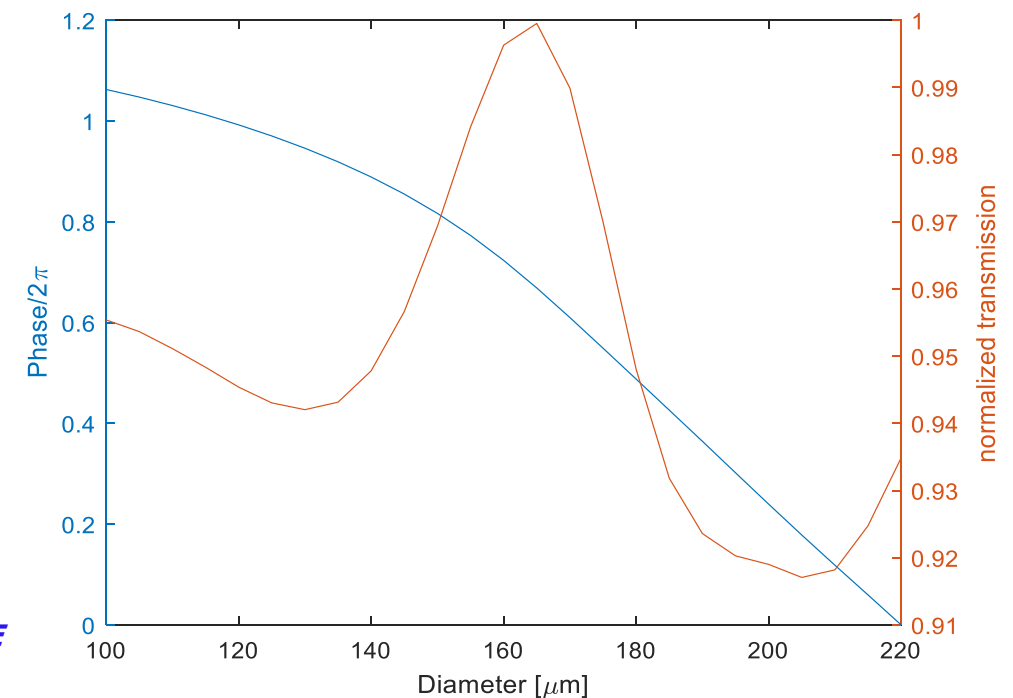
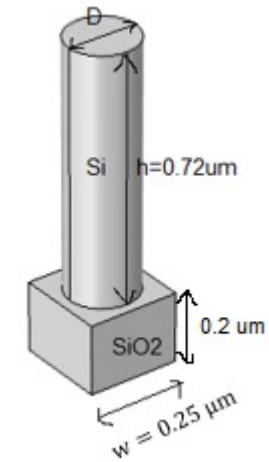


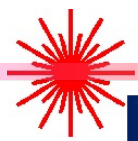
Fig.1 (a) 1D quadratic phase profile (b) Proposed system architecture



Meta-surface Building Block

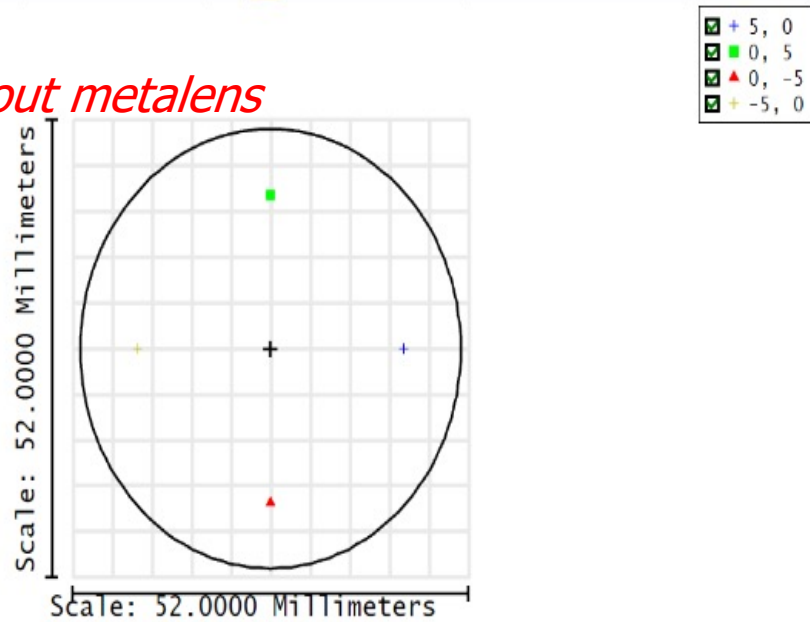
- a-Si nanopillar on SiO₂ substrate (Fig 4(a)) works as building block for metalens
- The separation between each building block remains fixed (0.25 μm) whereas the diameter is varied to realize full 0-2 π phase shift (Fig. 4(b))
- The design is highly transmissive, polarization insensitive and can be fabricated with existing fabrication process





Footprint Diagram for +/- 5 Incident Angle

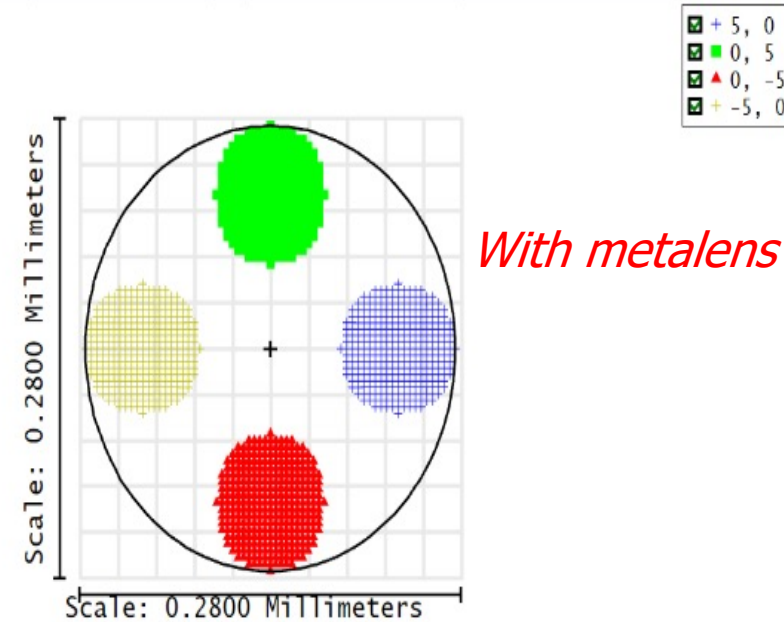
Without metalens



Aperture Diameter: 50.0000 % rays through = 100.00%

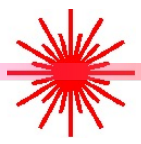
Footprint diagram on focal plane of first metalens shows that to capture incident angles up to ± 5 degree we need a detector of diameter 50 mm. The beam width on this plane is $\sim 127 \mu m$.

With metalens

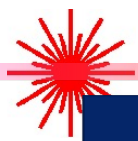


Aperture Diameter: 0.2714 % rays through = 100.00%

Footprint diagram on detector plane shows that to capture incident angles up to ± 5 degree we need a detector of diameter $271 \mu m$. The beam width is $\sim 82 \mu m$.



Multi-Tone Continuous Wave Lidar

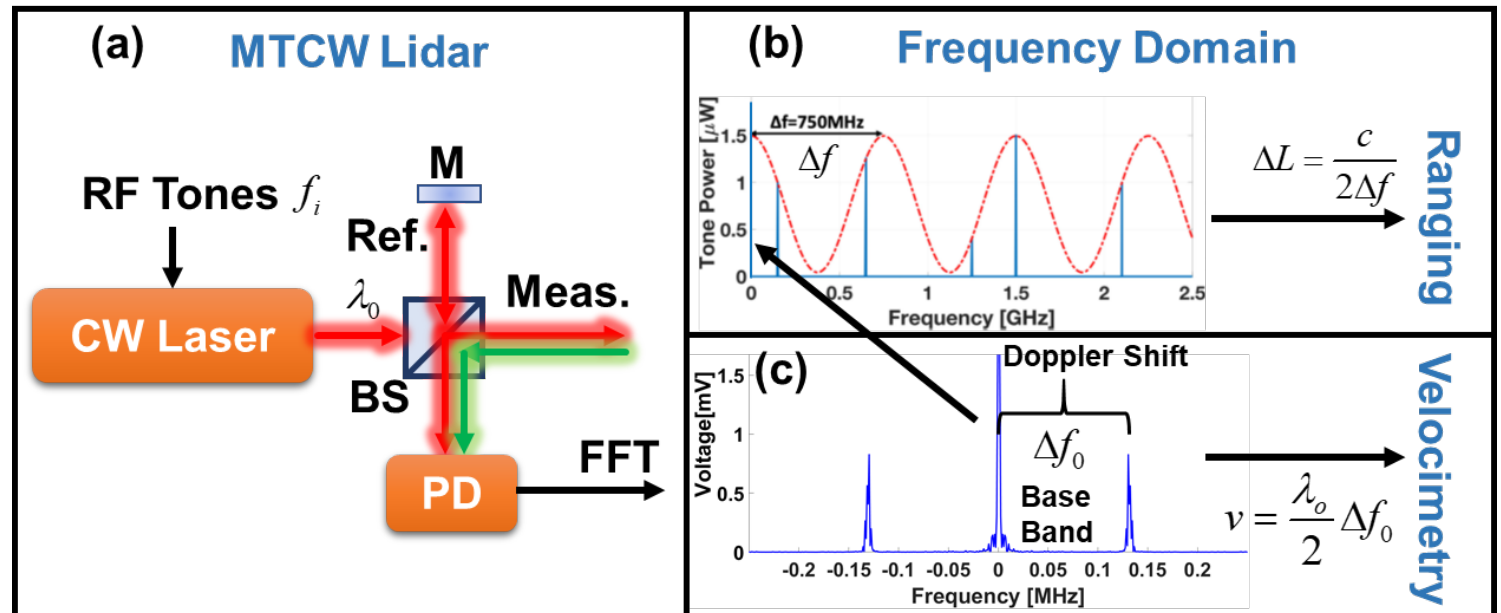


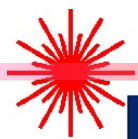
Motivation

- ❑ Is there a new LIDAR technique that can:
 - Enable single shot measurement by eliminating the need of
 - frequency sweeping
 - amplitude sweeping
 - phase sweeping
 - overcome coherence length limitations
 - Provide high precision simultaneous range and velocity measurement of static and moving targets
- ❑ These will allow to achieve single-shot range and velocity measurements unlike the other Lidar configurations.

What is MTCW Lidar?

- ❑ MTCW Lidar is a new method that can perform simultaneous ranging and velocimetry without any form of sweeping.
 - ❑ A single CW laser is modulated by multiple frequencies and split into two to achieve coherent detection similar to FMCW Lidar.
- Each frequency will accumulate a different phase.
 - The resultant tones will yield a sinusoidal pattern to acquire the range.
 - Doppler shift will yield the speed information.



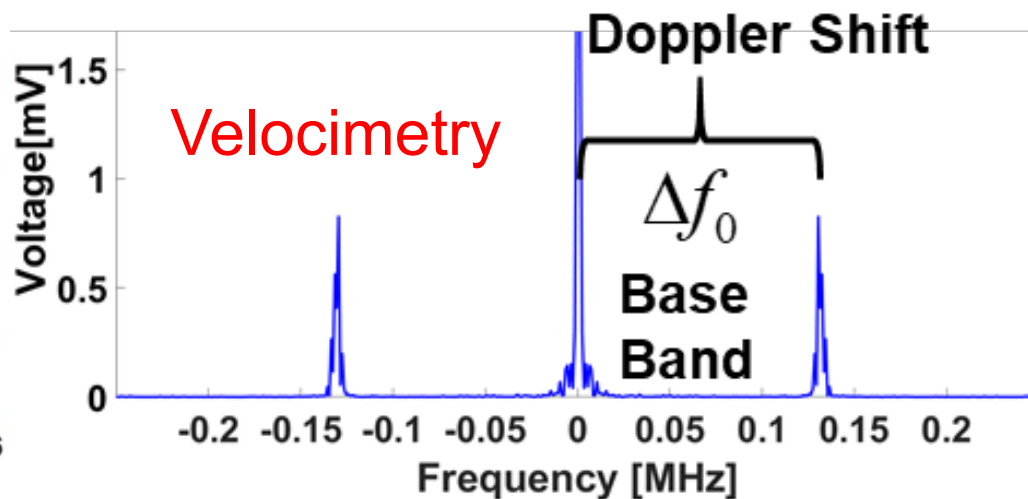
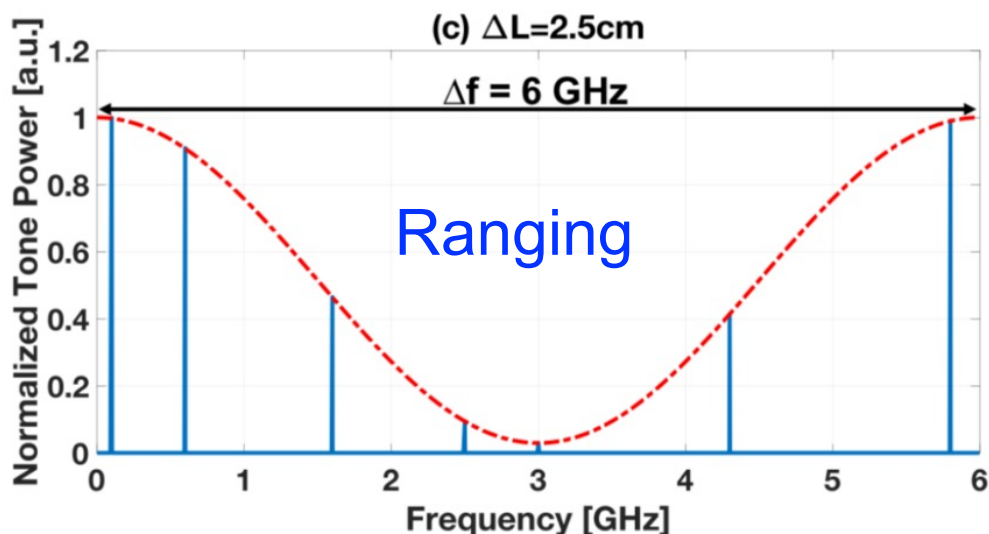


Principle – Simultaneous Ranging and Velocimetry

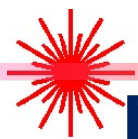
- For ranging, each **tone will have a different power** depending on the interference amount. Applying a **sine fitting and extracting the frequency** of the fitting curve can yield the range.
- The cross-tone beatings of the reference and measurement branches will create a frequency spike at the **Doppler frequency** near the base band that can yield the target speed.

$$\Delta L = \frac{c}{2\Delta f}$$

$$v = \frac{\lambda_0}{2} \Delta f_0$$

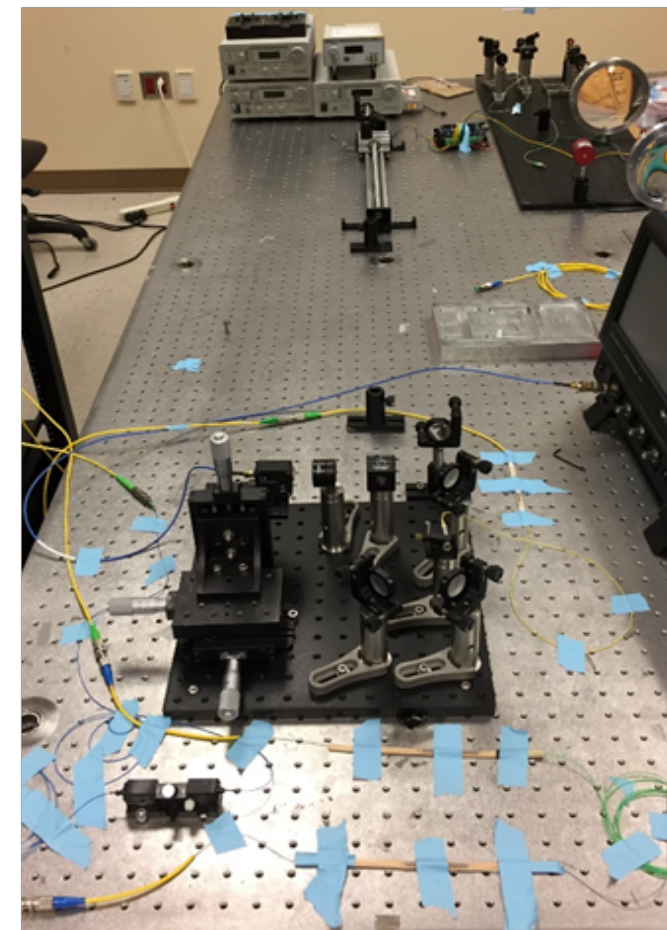
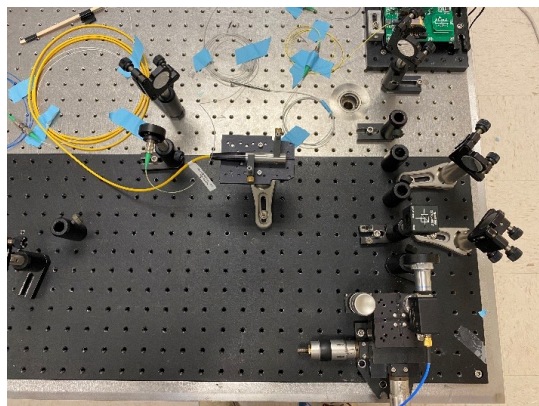
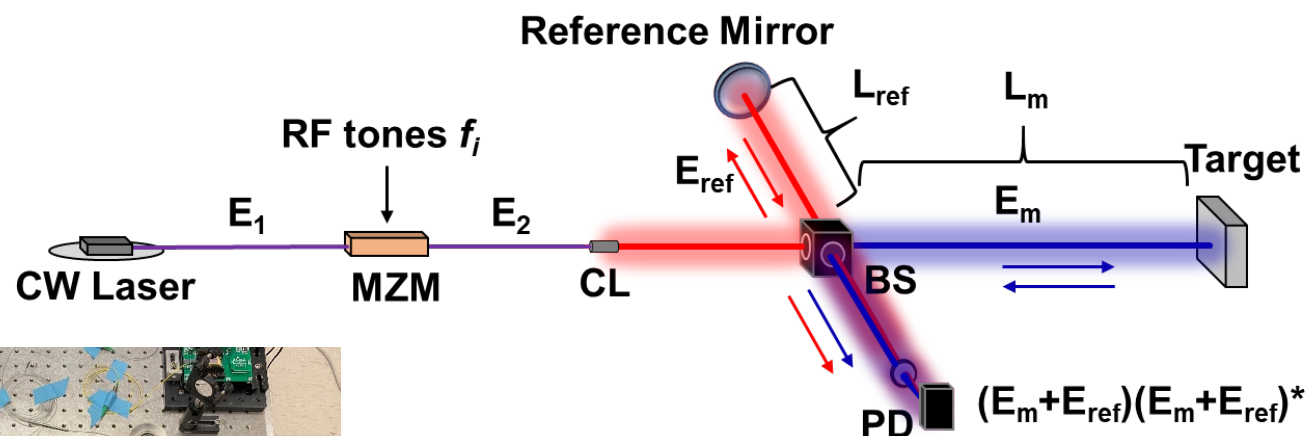


- Therefore, ranging and velocimetry can be performed simultaneously.



Experiments and Results: Amplitude Based

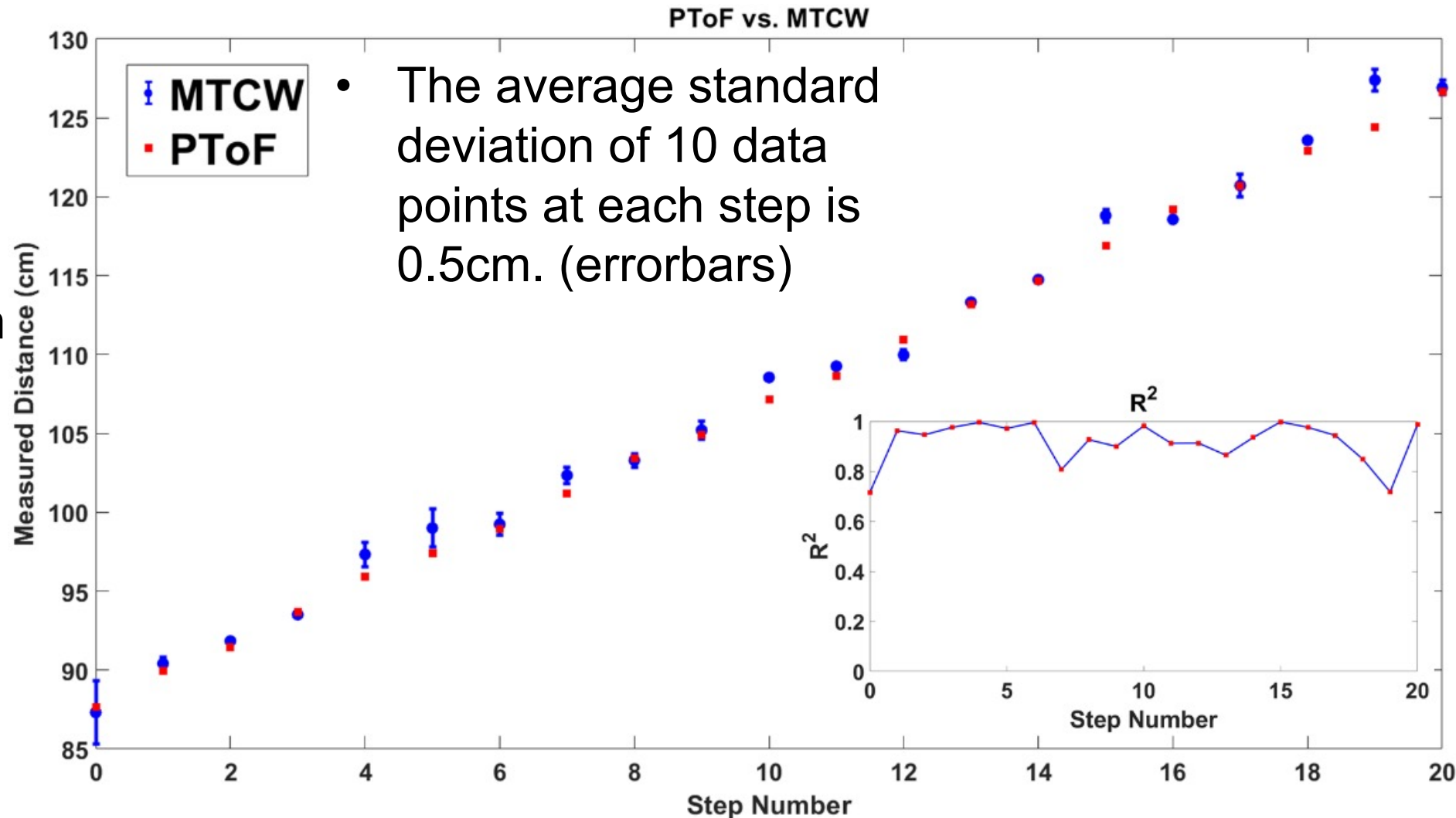
Stationary target PToF and MTCW comparison
Simultaneous Ranging and Velocimetry Experiment



1. R. Torun, M. M. Bayer, I. U. Zaman, J. E. Velazco, and O. Boyraz, "Realization of Multitone Continuous Wave Lidar," *IEEE Photonics Journal* **11**, 1–10 (2019).
2. R. Torun, M. M. Bayer, I. U. Zaman, and O. Boyraz, "Multi-tone modulated continuous-wave lidar," *Proc. SPIE* **10925**, 109250V (2019).
3. O. Boyraz, M. M. Bayer, R. Torun, and I. Zaman, "TuD2.2 - Multi Tone Continuous Wave Lidar (Invited)," in *IEEE Photonics Society Summer Topical Meeting Series* (IEEE, 2019), pp. 1–2.
4. M. M. Bayer, R. Torun, I. U. Zaman, and O. Boyraz, "A Basic Approach for Speed Profiling of Alternating Targets with Photonic Doppler Velocimetry," in *Conference on Lasers and Electro-Optics*, OSA Technical Digest (Optical Society of America, 2019), p. AW4K.4.

Ranging – PToF vs. MTCW Lidar

- The average mismatch between PToF and MTCW is $\sim 0.75\text{cm}$.
- The accuracy of PToF is also 0.75cm due to time resolution.
- R^2 is the statistical measure to show the goodness of the sine fitting.
- Average R^2 is 0.91 , $>90\%$ fitting accuracy.





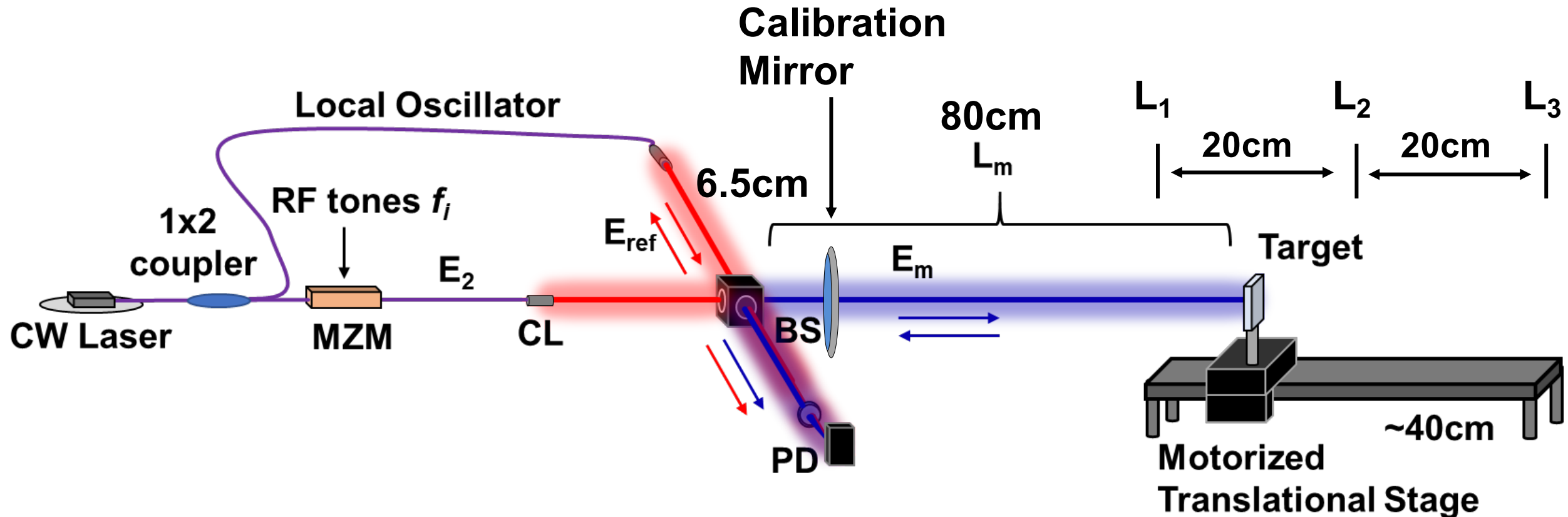
Theory: Phase Based

$$\begin{aligned}
 I_{PD} = & RA_0^2 \alpha_f \alpha_f^2 \beta + \frac{3RA_0^2 \alpha_m^2 \alpha_f^2 (1-\beta)}{16} + \frac{RA_0^2 \alpha_m \alpha_f^2 \sqrt{\beta} \sqrt{1-\beta}}{\sqrt{2}} \cos\left(\omega_0 \frac{2L_m}{c} + \phi_{L_1}\right) \\
 & - \frac{RmA_0^2 \alpha_m \alpha_f^2 \sqrt{\beta} \sqrt{1-\beta}}{2\sqrt{2}} \left[\sum_{i=1}^N \cos\left(\omega_i t + \phi_i + (\omega_0 + \omega_i) \frac{2L_m}{c} + \phi_{L_1}^i\right) + \sum_{i=1}^N \cos\left(\omega_i t - \phi_i - (\omega_0 + \omega_i) \frac{2L_m}{c} - \phi_{L_1}^i\right) \right] \\
 & + \frac{RmA_0^2 \alpha_m^2 \alpha_f^2 (1-\beta)}{8} \left[\sum_{i=1}^N \cos\left(\omega_i t + \phi_i + \omega_i \frac{2L_m}{c} + \phi_{L_1}^i - \phi_{L_1}\right) + \sum_{i=1}^N \cos\left(\omega_i t - \phi_i + \omega_i \frac{2L_m}{c} - \phi_{L_1}^i + \phi_{L_1}\right) \right] \\
 & + \frac{Rm^2 A_0^2 \alpha_m^2 \alpha_f^2 (1-\beta)}{8} \sum_{i=1}^N \cos\left(2\omega_i t + \omega_i \frac{4L_m}{c}\right)
 \end{aligned}$$

- Phase at each tone: $2 \cos\left(\omega_i t + \frac{2L_m}{c} \omega_i\right) \cos\left(\phi_i + \phi_{L_1}^i + \frac{2L_m}{c} \omega_0\right)$
- Phase and L_m :

$$\begin{aligned}
 \phi_m^1 &= 2\pi q + \frac{2L_m}{c} \omega_1 & \phi_m^1 - \phi_m^2 &= 2\pi n + \frac{2L_m}{c} (\omega_1 - \omega_2) \\
 \phi_m^2 &= 2\pi k + \frac{2L_m}{c} \omega_2 & \Delta\phi_{i,j} &= 2\pi n + \frac{2L_m}{c} (\Delta\omega_{i,j}) & L_m &= \frac{(2\pi n + \Delta\phi_{i,j})c}{\Delta\omega_{i,j}}
 \end{aligned}$$

Experimental Setup: Phase Based



- *Since exact phase of the local oscillator is not important, proposed method can allow ranging beyond the coherence length of the laser*

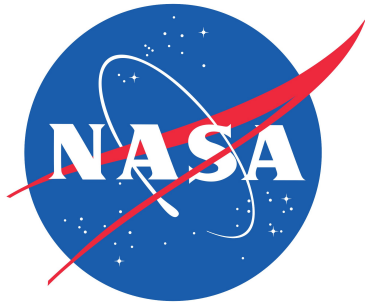
Acknowledgments

Funding agencies:

NASA Cooperative Agreement Partnerships with Universities (NNX16AT64A)

Office of Naval Research (N00014-18-1-2845)

University of California, Irvine (PhD Fellowship)



NASA SSTP Alumni: Rasul Torun, Ph.D. 2019
Imamuz Zaman, Ph.D. 2021
M. Mert Bayer, Ph.D., *continue*

For Detailed Questions: oboyraz@uci.edu or (949) 824 1979